IEEE Access
Multidisciplinary ⋮ Rapid Review ⋮ Open Access Journal

Received 6 October 2022, accepted 1 November 2022, date of publication 9 November 2022, date of current version 17 November 2022.

Digital Object Identifier 10.1109/ACCESS.2022.3220900

RESEARCH ARTICLE

A Wearable Solar Energy Harvesting Based Jacket With Maximum Power Point Tracking for Vital Health Monitoring Systems

ATIF SARDAR KHAN AND FARID ULLAH KHAN
Department of Mechatronics Engineering, University of Engineering and Technology Peshawar, Peshawar 25000, Pakistan
Corresponding author: Atif Sardar Khan (atifsardarkhan@uetpeshawar.edu.pk)

ABSTRACT Wearable sensors and electronic devices have gained a lot of attention during the last few years. The advances in low power wearable gadgets have the research venue in the field of energy harvesting to exclude or supplement the battery's power. Solar energy harvesting is a suitable source to power wearable gadgets. This work presents a wearable solar energy harvesting based jacket that can power the in-situ vital health monitoring system (VHMS). The developed VHMS comprised of sensors to measure several data and transferred through various Modules every 3 min with an emergency alert option. To integrate the Solar Energy harvester (SEH) and VHMS, a novel maximum power point tracking is designed, fabricated and tested to compensate the battery during diffused light as power is recorded to be as low as 7.95×10^{-5} mW at an optimal load of 10 kΩ. Ten flexible solar cells (each 146 mm × 167.5 mm in size) placed each inside a transparent pouch stitched to a jacket. An individual and series configuration of all solar cells is tested in-lab and outside in real environment under different illuminance and irradiance. At an optimal load resistance of 1.5 kΩ, the developed self-powered, smart jacket is capable to generate a voltage of 45 V and power of 1282.57 mW, under lights' illuminance of 41000 lux and irradiance of 780 W/m^2. The proposed SEH has been validated through a prototype system. Its performance compares favorably against various solar energy harvester for wearable sensors based on size, power, modes to communicate and sensors.

INDEX TERMS Arduino based, biomedical gadgets, Bluetooth module, GSM module, self-powered, solar energy harvester, smart jacket, vital health monitoring system, Wi-Fi module, wireless sensor nodes.

I. INTRODUCTION

Since last decade, the usage of wearable gadgets, biomedical sensors and portable electronic devices have been rapidly increasing and the development is not just limited to prototyping but also the product is commercially available worldwide. For example, in 2019, almost 25 billion dollars of revenue [1] is produced with sales of these wearable products. Wearable electronic products' emergence is applicable to fields, like, health care monitoring [2], sports [3], entertainment [4], human machine interface [5], artificial skin [6], human motion monitoring [7], and industrial application [8]. The manufacturing of wearable electronic products is growing fast and capturing the market to provide the monitoring, communication and data analysis capabilities to a human body. These wearable sensors (WS) are worn or attached to human body for directly providing the relevant information on spot or remotely communicated through internet of things (IoT) technology. The WS's collect the physiological data throughout the day which is not easily achievable with the stagnant laboratory equipment. Due to robustness, the interest of users in utilizing these wearable devices is swiftly increasing as shown in Table 1. As depicted in Table 1, commercially available wearable devices and gadgets are covering most of the applications trending now a days and the technology is also rapidly in use, like, wearable devices now include, smart watches, wristbands, smart eye wears, headsets, ear buds, smart jewelry, straps, smart garments, foot/hand worn gadgets, smart patches, e-tattoos and so on. The wearable devices mostly use Lithium battery for powering different

The associate editor coordinating the review of this manuscript and approving it for publication was Diego Masotti.

TABLE 1. Main parameters of commercially available wearable devices and gadgets.

Wearable devices	Sensor's availability	Battery type	Operation time	Communication node	Activity	Commercially available products	Ref.
Wrist-worn							
Smart watches	Accelerometer, gyroscope, heart rate monitor, barometer, ambient light sensor and heart rate sensor	Li-Poly/300 mAh	1.5 days	Bluetooth 4.0, Wi-Fi (802.11b/g/n 2.4 GHz) and NFC	Digital assistant and measure different subject activities	Moto 360 Huawei Watch (42 mm)	[10] [11]
Wrist bands	Accelerometer, optical heart rate sensor, Location tracking sensors	Li-Poly	5 days (10 hrs with GPS)	Bluetooth 4.0	Measure different subject activities	Fitbit Flex	[12]
		Li-Poly/70 mAh, 20 days	20 days			Mi Band 2	[13]
Head-mounted devices							
Smart eyewear	Accelerometer, gyroscope, magnetometer, pressure sensor, infrared (IR) sensor, Bone conduction transducer, ambient light sensor, proximity sensor, touchpad, camera.	Li-ion/570 mAh		Wi-Fi 802.11b/g, Bluetooth, micro-USB	Sensing, transceiver for data transfer	Google glass	[14]
		Li-ion, 4 hrs	4 hrs			Recon Jet	[15]
Headsets and Ear-buds	Proximity, Gyroscope, Optical heart-rate sensor & 3-axis accelerometer		24 hrs (with charging case) and 5 hrs in one charge	Bluetooth, charging case, NFC and Bluetooth 4.1	Bluetooth enabled	Apple AirPods	[16]
Other Accessories							
Smart Jewelry		Replaceable coin	6 months	Bluetooth	Health-monitoring	Bellabeat Leaf	[17]
Straps	3-axis accelerometry, electrocardiography	Micro-USB charging, built-in rechargeable lithium-ion battery	1 day	Bluetooth 4.0	Bands or straps equipped with sensors for health tracking	MYO Armband	[18]
Foot/Hand-worn	Count actual steps	USB charging		Bluetooth	wearable sensors for monitoring purpose	Lechal	[19]

sensors as accelerometer, gyroscope, heart rate monitor, barometer, ambient light sensor and heart rate sensor, location tracking sensors, pressure sensor, infrared (IR) sensor, electrocardiography, and actual count step etc. These sensors data can be communicated using several methods of communication like NFC, Wi Fi and Bluetooth. The market of wearable devices is expected to be $57,653 million by 2022 [9].

TABLE 2. Ambient energy sources and power scavenging techniques available for energy harvesting.

Harvesting Method	Harvesting Condition	Voltage range	Power Density		Ref.
		(V)	(μW/cm^2)	(μW/cm^3)	
Solar Cell (Si)	Day time	0.5	15000		[30]
Solar Cell (a-Si)		1			
Radio frequency (GSM)	Patch antenna		0.001-0.1		[31]
Thermal	ΔT = 5 ºC		35		[32]
Electromechanical conversion	Wind flow and hydro			16.2	[33]
Piezoelectric	Acoustic Noise			0.96	[33]
	Motion			330	[34]

Mostly wearable devices require batteries to power the onboard sensors, electronics and communication and display modules. However, the limited life-span of batteries made the wearable device much more unreliable and therefore, an alternate, more durable and a lifetime energy source is required for their operation. Usually this issue, nowadays, is resolved by integration of an energy harvester as a supplement power source in wearable devices [20]. Various wearable energy harvesters (WEHs) are utilized for wearable gadgets and biomedical sensors, such as, triboelectric [21], thermoelectric [22], piezoelectric [23], [24], electromagnetic [25], [26], electrostatic [27], radiofrequency (RF) [28] and solar [29] energy harvesters.

As can be seen in Table 2, an ambient solar energy source is available where a direct sunlight power density is sufficient to operate the wearable device. Even for a solar cell the power density is 15000 μW/cm^2 which is quite enough to power wearable bio-medical sensors and electronic gadgets. Table 2, shows that among the available energy sources, performance of solar cell is better than any other energy source. Moreover, in terms of power density, no other ambient energy source is even close to the solar energy harvesting which makes it the most suitable and demanding energy-harvesting source to be utilized for commercial product development.

Harvesting from ambient energy sources, almost eradicates the use of battery, which has a limited life span and hazardous to environment. Recently solar energy harvesters (SEHs) are being utilized to operate the wearable sensors and biomedical portable gadgets.

Moreover, the combination of solar cells can easily generate reasonable power to operate wearable devices and biomedical sensors or any wearable gadget. The solar cell current is dependent on the illumination (mW/cm^2) and the active area of cell. For protection, the top surface of a solar cell is encapsulated with a glass window [35].

Several solar energy harvesters (SEHs) based self-powered wearable devices and gadgets have been developed and reported in literature. Taiyang Wu et al. developed a SEH based flexible wearable sensor [36] to measure heartbeat of a subject. A flexible PCB is used for sensor node connectivity with a flexible solar cell (60 mm $\times$ 72 mm). The system can easily be attached to a human body. The SEH produced a voltage and power of 5.08 V and 127.8 mW respectively to charge a 12.5 F super capacitor. The developed wearable bracelet [37] utilizes a

SEH as an energy source for the measurement of blood oxygenation and sending the measurement per min via a Bluetooth connectivity. For a flexibility of this monitoring system, the entire gadget is assembled on a polyamide film. The maximum power of around 18 mW at 10000 lux and 0.21 mW in indoor condition is produced with the reported SEH. In [38], a novel SEH fabric is developed to power wearable and mobile devices. The combination of 200 solar cells (44.5 mm $\times$ 45.5 mm active area), are connected within a fiber of a textile yarn. The design helps to keep flexibility and deformability. Experimentation results are achieved under different light intensities and incident light angles. The SEH is capable to produce a power, power density, open-circuit voltage and short-circuit current of 43.4 mW, 2.15 mW/cm^2, 5.14 V and 14.14 mA respectively. V. Kartsch et al. reported a fully-flexible low-power wristband [39] which has several components for the detection of five hand gestures from four Electromyography (EMG) sensors. The device is self-powered by SEH. Experimental measurements indicated that the energy harvesting subsystem using a single flexible cell can provide up to 0.21 mW, during indoor and up to 16 mW of power in outdoor scenarios.

Taiyang Wu et al. [40] developed a SEH system with a maximum power point tracking (MPPT) algorithm for a pulse sensor. The reported device can transmit the data through a Bluetooth. The experimental results demonstrated that the charging efficiency of the solar energy harvesting system is 66.5 % and is capable of generating a voltage of 2.7 V, and power of 120.7 mW. A self-powered prototype [41], is developed for a wearable, biomedical applications, which is comprised of a flat and bent solar cell. The SEH of size 60 mm $\times$ 72 mm is placed under solar light of 320 lux, which produced 77 μW of power. A wearable SEH is fabricated based on perovskite solar cells [42] for applications of electric watch. It has been reported that large perovskite crystals and aligned carbon nanotube sheet combined for excellent performance. The size of device was 1 $\times$ 5 mm^2 and it produced an open-circuit voltage of 0.91 V, short-circuit current of 15.9 mA/cm^2 and a fill factor of 0.656.

Several proposed devices are reported in literature but due to small size of a solar cell countable sensors are powered. Moreover, the performance of solar cells is degraded in diffused light even after integration of maximum power point tracking (MPPT) circuit. Furthermore, the mode of communication is limited due to limited power source but in our proposed device all these limitations are overcome, as the device work in diffused light, unlike prior work. Moreover, several sensors such as PPG, Temperature and accelerometer sensors are used whereas, for communication Bluetooth, GSM and Wi-Fi modules modes are utilized.

This paper investigates a vital health monitoring system (VHMS) based self-powered wearable jacket. Flexible, light weight solar cells are attached to the front and back of the jacket to act as SEHs for powering the wearable sensor, relevant electronics and the communication modules. In the developed jacket, ten transparent zip pouches, six on front and four on back side are produced to contain the flexible solar cells. The utilization of flexible solar cells in the prototype does not compromise the comfort of wearer, and are capable of producing enough power for VHMS operation. Moreover, to achieve high output voltage and power during different environmental conditions, and varying load situation, a novel MPPT circuit is designed and fabricated to improve the performance of devised SEH based VHMS during diffused light in the jacket. Various scenarios are considered for powering sensors from PV cells. Both natural and artificial lights are utilized to justify the working of MPPT circuit which, due to its simplified and efficient operation, is able to operate under diffused and day light. A developed MPPT circuit design enhances the performance of energy harvesting technique by utilizing even the ultra-low power in diffused light conditions. The operation of this technique is verified to power a wearable VHMS attached to the jacket. Additionally, in the jacket through a VHMS the subject data is monitored and remotely transferred to mobile application, web database, Bluetooth and through mobile message.

II. DEVELOPMENT OF A VITAL HEALTH MONITORING SYSTEM (VHMS) BASED SELF-POWERED WEARABLE JACKET

As shown in figure 1, the developed self-powered wearable jacket is composed of three subsystems, comprising of a vital health monitoring system (VHMS), power management circuit and a solar energy-harvesting unit. VHMS include of sensors and transmission modules (figure 1(a)). Initially, human oxygen level, blood pressure, pulse rate and temperature data are collected and transmitted through Bluetooth, GSM and Wi-Fi modules. Furthermore, VHMS is integrated to a power management circuit which has a potential even to route low voltage energy during diffused light. The power management circuit comprise of a dc-to-dc boost and dc-to-dc buck converter. During day light, dc-to-dc buck converter will regulate high voltage produced by a SEH and an ultra-low voltage produced by a solar energy harvester is amplified by dc-to-dc boost converter to compensate a rechargeable battery during diffused light. The entire circuitry is powered by a wearable SEH. A SEH includes ten solar cells inserted inside stitched transparent pouches, where the solar cells can be connected in series/parallel depending upon the requirement of the system.

Furthermore, the developed VHMS based self-powered wearable jacket is shown in figure 1(b). In a normal fabric jacket, ten pouches of transparent plastic material are stitched according to size of AT-7963A SEH module. The pouches protect and hold the SEH module as well as add aesthetics to the jacket without compromising on the comfort to the wearer. One AT-7963A SEH module is placed inside each pouch. Six pouches are kept on front of the jacket (three on each side) and four on the back side. In the prototype, the number of AT-7963A SEH cells (each have a size of 146.0 mm $\times$ 167.5 mm) are considered based on the available area of jacket and power requirements of the wearable electronics. Moreover, the SEH modules are not permanently fixed and can be easily disconnected and disintegrated from the jacket. Even the number of SEH modules can be increased or decreased depending upon the requirement. Additionally, the wearable SEH jacket is completely portable and easy to wear.

III. VITAL HEALTH MONITORING SYSTEM FOR WEARABLE JACKET

The VHMS on the jacket is consisted of an Arduino (nano nodemcu) interfaced with a Wi-Fi module, Bluetooth module (HC-05), GSM900 module, SpO_2 sensor (MAX30102), temperature sensor (Thermistor 10k), pulse sensor (MAX30102) and accelerometer (ADXL335). Sensors' data is transferred every 3 min through Wi-Fi and GSM module to mobile phone and laptop. A Wi-Fi module transfers data both to computer and mobile phone whereas, GSM module is communicating through a mobile phone. In case of an emergency, if the pulse, oxygen saturation or temperature reading is not in a normal range, an emergency message is to be sent to a mobile phone

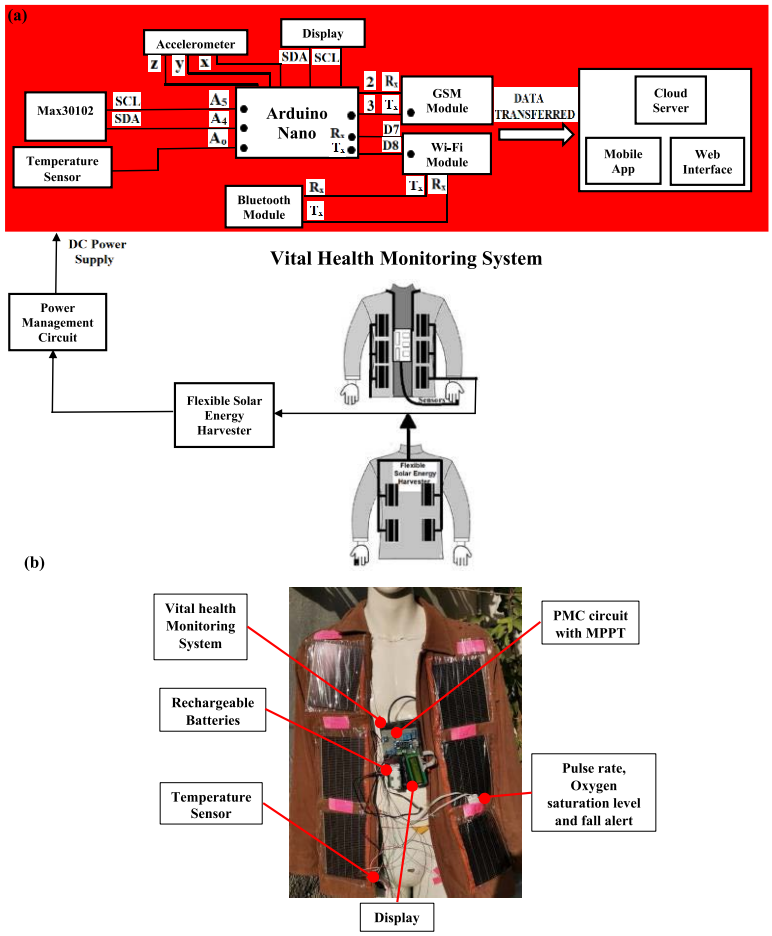

FIGURE 1. Vital health monitoring system based self-powered wearable jacket: (a) Schematic diagram and (b) developed prototype of a VHMS based self-powered wearable jacket.

and laptop. The detail of sensors and modules used in the devised VHMS is given in table 3.

The total power consumption

$$P_t = P_{alot} + P_a + P_{gwb} \tag{1}$$

Of the developed VHMS prototype can be estimated from the power consumption of accelerometer, LCD display, oximeter, pulse rate sensor and thermistor P_{alot}; power requirement of Arduino P_a; and the power consumption of GSM module, Wi-Fi module, and Bluetooth module P_{gwb}.

In the VHMS all modules are dynamic and are defined by the duty cycle activity between operation modes and sleep mode. After every 3 min, these modules wakeup into active mode to retrieve data from sensors and transmit the information to smart phone, laptop, web and mobile application.

Since, the wakeup mode of GSM module occurs after every 3 min, while the wakeup time $T_{ws} = 3$ sec (for every sleep mode time, $T = 3$ min), therefore the duty cycle

$$D = \frac{T}{T_{ws}} = 0.0167$$

Can be used to compute the wakeup current of GSM, Wi-Fi and Bluetooth modules by multiplying it with a transmission module current and is further added to the sleep mode current for the total current consumed by each module. The total current consumed by the modules is when multiplied by the operating voltage, the total power

$$P_{gwb} = P_g + P_w + P_b \tag{2}$$

Consumed by the GSM, Bluetooth and Wi-Fi modules can be estimated.

Calculates the power consumption of modules which is $P_{gwb} = 68.22$mW for equation (2) and the total power, P_t consumed is $P_t = 91.826$ mW.

A. DEVELOPMENT OF A POWER MANAGEMENT CIRCUIT FOR A SELF-POWERED JACKET

The design of the devised maximum power point tracking (MPPT) with buck and boost converter is based on two different circuit chips, namely the DC-DC buck converter (YS-04) and an ultra-low-voltage boost converter (ECT310). Both Integrated Circuit (IC) chips are power management circuits. The ECT310 has acceptable extreme low input voltage (as low as 20 mV). As diffused light intensity energy is usually wasted, however, with the integration of ECT310 in

TABLE 3. Sensors and modules used in wearable vital health monitoring system.

Sensors/Modules	Type	Model	Measurement	Operating Voltage (V)	Electrical Current consumed (mA)			Power Consumed (mW)		
					Sleep mode	Transmitting mode	Total	Sleep mode	Transmitting mode	Total
Accelerometer	Sensor	ADXL335	Subject fall sensor	1.8 – 3.6					0.63*	
High Sensitive Oximeter and pulse-rate	Sensor	MAX30102	Pulse rate and Oxygen saturation level	1.8 – 3.3				< 1		
Thermistor	Sensor	Thermistor 10k	Subject Temperature					0.042		
LCD Display				4.7 – 5.3	1			0.0047		
Arduino	Module	Nano	Receive sensors' data and transmit through modules	5				45		
GSM	Module	SIM 900 GSM	Sending the notification through a text message to the Emergency center	V_g = 3.2 – 4.8	I_{sm} = 1	I_{tm} =150	I_g = 3.505	3.2*	480*	P_g = 11.216
Wi-Fi	Module	ESP8266	Receives data of sensors through Arduino and transmits it to the cloud server, mobile app and web interface	V_w = 3.3	I_{smw} = 15	I_{tmw} = 100	I_w = 16.67	49.5*	330*	P_w =55.01
Bluetooth	Module	HC-05	For exchanging data wirelessly over short distances	V_b = 4 – 6	I_{smb} = 6.4	I_{tmb} = 30	I_b = 6.9		120* 120**	P_b = 2

***calculated** ****pairing mode**

TABLE 4. Main electronic component used in integration of MPPT with buck and boost converter.

Circuit part	Model type	Efficiency (%)
Zener diode	1N4731A	
Ultra-low voltage regulator	EnOcean ECT-310	30*
Relay	Songle 5 VDC	
DC-DC converter buck module	YS-04	86
Diode	2N2222	
Diode	1N4007	
Resistor	1kΩ	

* At as low as 25 mV input voltage

the VHMS, the diffused light can also be harvested for use. A schematic and a photograph of the developed prototype MPPT can be seen in figure 2(a) and figure 2(b) respectively, whereas its main components are listed in Table 4.

1) START-UP AND WORKING PRINCIPLE OF MPPT

Initially, when the system has not started up and the SEH is connected to the MPPT circuit, a Zener diode (1N4731A) turns ON at 4.3 V, therefore at the moment when the voltage is below 4.3 V, the Zener diode will not operate and the DC-DC converter ultra-low voltage regulator (EnOcean ECT-310) will turn ON to produce 5 V to recharge the battery. In case the input voltage increases above 4.3 V it will instantly turn ON the Zener diode, a Darlington pair as shown in figure 2(a), and a relay. A 1N4007 diode is a free wheeler diode which avoids back electromotive force caused by a relay coil. This way, in response, a DC-DC converter (YS-04) operates to regulate a voltage range from 4.5 V – 40 V to 5 V. The MPPT circuit works both during a diffused and normal light condition to compensate charging capability of a rechargeable battery in order to power the VHMS.

B. SOLAR ENERGY HARVESTER FOR SELF-POWERED WEARABLE JACKET

For the development of a VHMS based self-powered wearable jacket, flexible amorphous silicon solar modules (AT-7963A) are utilized as SEH. An advantage of using AT-7963A module is that it is flexible, efficient and comfortable to be implemented in wearing cloths. Table 5 shows the main features of AT-7963A SEH module.

An equivalent electrical circuit for a single solar cell module is shown in figure 3. In the equivalent circuit, the solar cell is represented by a current source I_{ph}, diodes saturation current (I_s), short circuit current (I_{sc}) , series resistance (R_s) and shunt resistance (R_{sh}) [43].

According to Kirchoff's current law, the load current [44]

$$I_L = I_{ph} - I_d - I_{sh} \tag{3}$$

TABLE 5. Properties of AT-7963A SEH module [53].

Items	Specifications
Solar cell model	AT-7963A
Brand	Sanyo
Type	Amorphous silicon solar cell
Dimension	146 mm × 167.5 mm
Effective Area	138.8 mm × 165.6 mm
Module Thickness	0. 3 mm
Working temperature range	-10 to +60 °C*

***Solar simulator results**

Pass through the load can be obtained with the photo current I_{ph}, diode saturation current I_d and shunt current I_{sh}

$$I_L = I_{ph} - I_d - \left(\frac{V_L + I_L R_S}{R_{sh}}\right) \tag{4}$$

Moreover, equation (2) is further expressed by expanding the diode saturation current

$$I_d = I_s \left\{\left(exp\left(\frac{q\,(V_L + I_L R_S)\,V_d}{kT_c A}\right) - 1\right)\right\} \tag{5}$$

Therefore, as a diode current acts as a current controlled current source in figure 3(b). Hence, the circuit can then be re-written as [45], [46], [47]

$$I_L = I_{ph} - I_s\left[exp\left(\frac{q\,(V_L + I_L R_S)}{kT_c A}\right) - 1\right] - \frac{V_L + I_L R_S}{R_{sh}} \tag{6}$$

where,

I_L = Output current, I_{ph} = Photo current, I_d = Diode saturation current, V = Voltage, R_s = Series resistance, R_{sh} = Shunt resistance, q = Electron charge = 1.6 x 10^{-19}C, k = Boltzman constant = 1.3805 x 10^{-23} J/K, T_c = cell temperature, A = Ideality factor

Whereas, photocurrent is the current gotten from the intensity of solar radiation. It is dependent on the solar intensity level and temperature. Also referred as the illuminated current and is given by [47] in equation (7)

$$I_{ph} = [I_{sc} + k_i(T - T_n)]\,\frac{G}{G_n} \tag{7}$$

where, G = Solar irradiance, G_n = Nominal solar irradiance at 1000W/m^2, T = Cell temperature, T_n = Nominal Temperature, k_i = Temp. Coefficient of short circuit current, I_{sc} = Short circuit current

When terminal of a solar cell is short circuited, V = 0, then a short circuit current grows linearly with the illumination intensity [48], [49], [50]

$$I_{sc} = I_{ph} - I_s\left[exp\left(\frac{I_{sc}R_s}{n \propto}\right) - 1\right] - \frac{I_{sc}R_s}{R_{sh}} \tag{8}$$

If a short-circuit current, I_{sc}, and the photo current, I_{ph}, are approximately identical, then the short-circuit current is the largest which may be withdrawn from the solar cell. Further

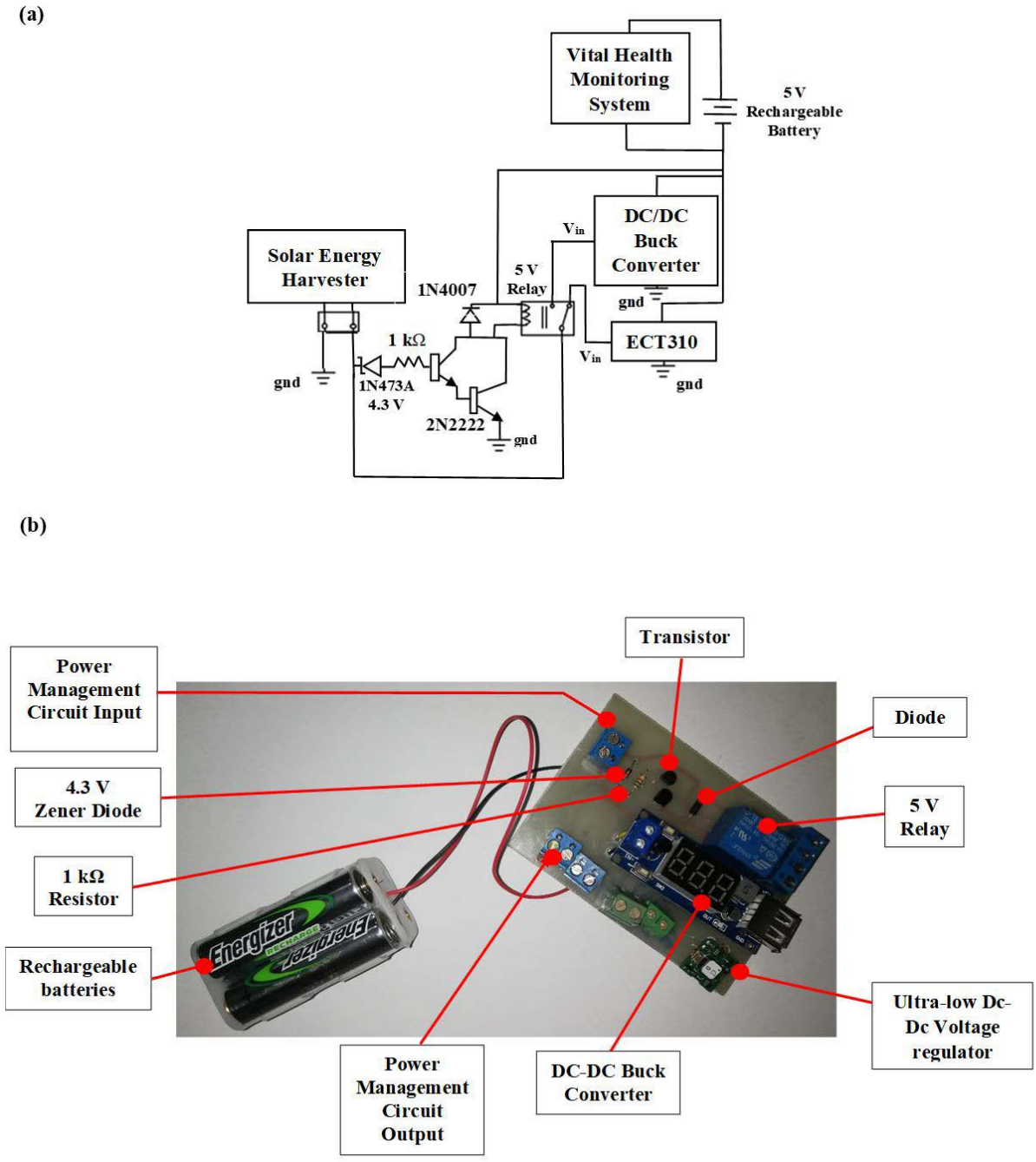

FIGURE 2. Power management circuit (a) schematic and, (b) photograph of a MPPT (including buck and boost converter) control circuit.

assume if R_{sh} is much greater than R_s, and I_s is smaller as compare to I, then:

$$I_{sc} \approx I_{ph} \tag{9}$$

Similarly, an open-circuit voltage is obtained when no current flows through the external circuit. The open circuit voltage depends upon the barrier potential of a junction and shunt resistance. Whereas, a decrease is seen in an open circuit voltage with an increase in temperature and light intensity has an impact too [43], [51], [52]. For $I_L = 0$,

$$0 = I_{ph} - I_s \left[exp\left(\frac{qV_{oc}}{kT_C A}\right) - 1 \right] - \frac{V_{oc}}{R_{sh}} \tag{10}$$

Finally, power delivered by the PV cell is the product of voltage (V) and current (I). At both open and short circuit conditions the power delivered is zero.

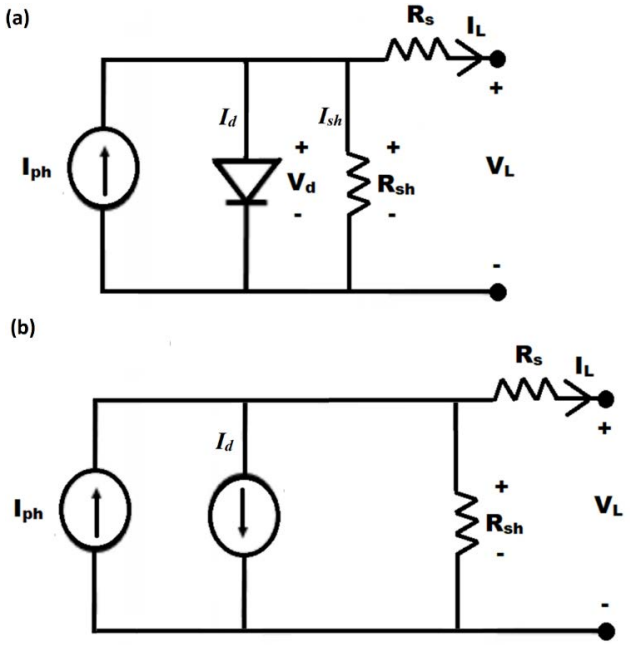

FIGURE 3. (a) Equivalent electrical circuit for a solar cell module (b) diode acting as a current source.

IV. EXPERIMENTATION OF SEH JACKET FOR INDOOR AND OUTDOOR LIGHTING CONDITIONS

For performance evaluation of SEHs embedded in the jacket, a dummy is used as a subject to conduct the experimentation. During indoor (in-lab) experimentation as shown in figure 4(a) and figure 4(b), a dummy wearing a SEH jacket is initially placed in a diffused light and afterward the illuminance is gradually increased by turning ON tube lights (from 1 to 16) inside the room to characterize the performance of prototype jacket. Similarly, during outdoor experimentation figure 4(c) and figure 4(d), a dummy having a SEH jacket is put on roof top and the operation of SEH is evaluated at 9 am, 4 pm, 6 pm and 8 pm. Moreover, individual solar modules, as well as, solar modules in series configuration are tested and characterized for both scenarios (i.e., indoor and outdoor). The output voltage, output power, illuminance and irradiance are measured through multimeter, lux meter and solar power meter respectively during indoor and outdoor experimentation.

A. IMPACT OF INDOOR DIFFUSED LIGHT AND LIGHT INTENSITY VARIATION OVER OPEN-CIRCUIT VOLTAGE OF PROTOTYPE

In the month of February around 11 am experimentation for diffused light in lab (no tube light is kept ON) is performed. Experimentation is performed to evaluate solar cells power generation capability during diffused light for a design of maximum power point tracking circuit (MPPT). The design and integration of MPPT circuit will further improve the performance by utilizing diffused light to compensate battery while powering vital health monitoring system (VHMS). Individually each solar cell is analyzed for output voltage and power for different intensity of diffused light. The front side of the jacket is facing the window from where the diffuse light is coming to the room. The orientation of the room is such that no direct solar radiations can enter the room through windows and doors. During the testing the dummy is place such that the front of the jacket is facing the windows. The maximum open circuit voltage of 2.87 V is produced by front side solar cell-5 whereas, 1.8 V is produced by solar cell-8, As shown in figure 5(a) and figure 5(b), the voltage varies between 2.18 V to 3.34 V for front-side of the jacket and on back-side the voltage ranges between 2.6 V and 3.04 V.

The measurement of the irradiance is between 0.4 W/m^2 to 1.1 W/m^2 on front-side and 0.4 W/m^2 to 0.5 W/m^2 on back-side of a jacket. Whereas, the illuminance varies between 15 lux to 18 lux for front-side of the jacket and 7 lux to 11 lux on back-side of the jacket.

The experimentation on wearable SEH based jacket is performed indoor during fall season. The testing in the lab is conducted under artificial lighting arrangement that is, turning ON 1 to 16 tube lights one by one (for variable lighting conditions). Each solar cell is individually evaluated based on voltage and power during available illuminance and irradiance on each solar cell. The illuminance and irradiance are recorded near each solar cell while keeping the sensing probes in plan (parallel) to solar cells. Figure 5(c) shows the individual solar cell's output open-circuit voltage for indoor experiments, while managing different light conditions using 1-16 tube lights, meanwhile, illuminance is measured to be 197 lux. For a single tube light, maximum open-circuit voltage attained is from 1.6 V to 2.81 V (illuminance from 8 lux to 24 lux). Whereas, for 16 tube lights (illuminance varies between 180 lux to 196 lux), the open-circuit voltage ranged between 2.18 V to 3.34 V. The maximum recorded voltage is 3.34 V for a solar cell-3, when all 16 tube lights are turned ON.

It is important to mention that voltage and power at the front is more than the back side of wearable SEH based jacket due to the fact that the front of the jacket is facing window, whereas back side is facing the wall. The same reason restricted the illuminance to 13 lux on solar cell-9 (back-side). Exploring another aspect, and to have more in-depth knowledge of a developed wearable SEH jacket prototype, an irradiance is also recorded as depicted in figure 5(d). The voltage increased with the controllable illuminance. When 1 tube light is turned 'ON' the maximum voltage on front-side of the jacket is produced by solar cell-3 and on back-side of 2.56 V is produced by solar cell-10. The voltage increases as the illuminance and irradiance is increased due to turning ON tube lights (as shown in figure 5(c) and figure 5(d)). When all the 16 tube lights are turned 'ON' in the room, the maximum voltage on front side solar cell-3 reaches 3.34 V and on back-side 3.04 V is produced by solar cell-10. Due to turning 'ON' the tube lights one by one the irradiance on front-side and back-side of the jacket is increased to 2.7 W/m^2 and 0.4 W/m^2, respectively. The front-side six solar cells voltage is more than that of back-side solar

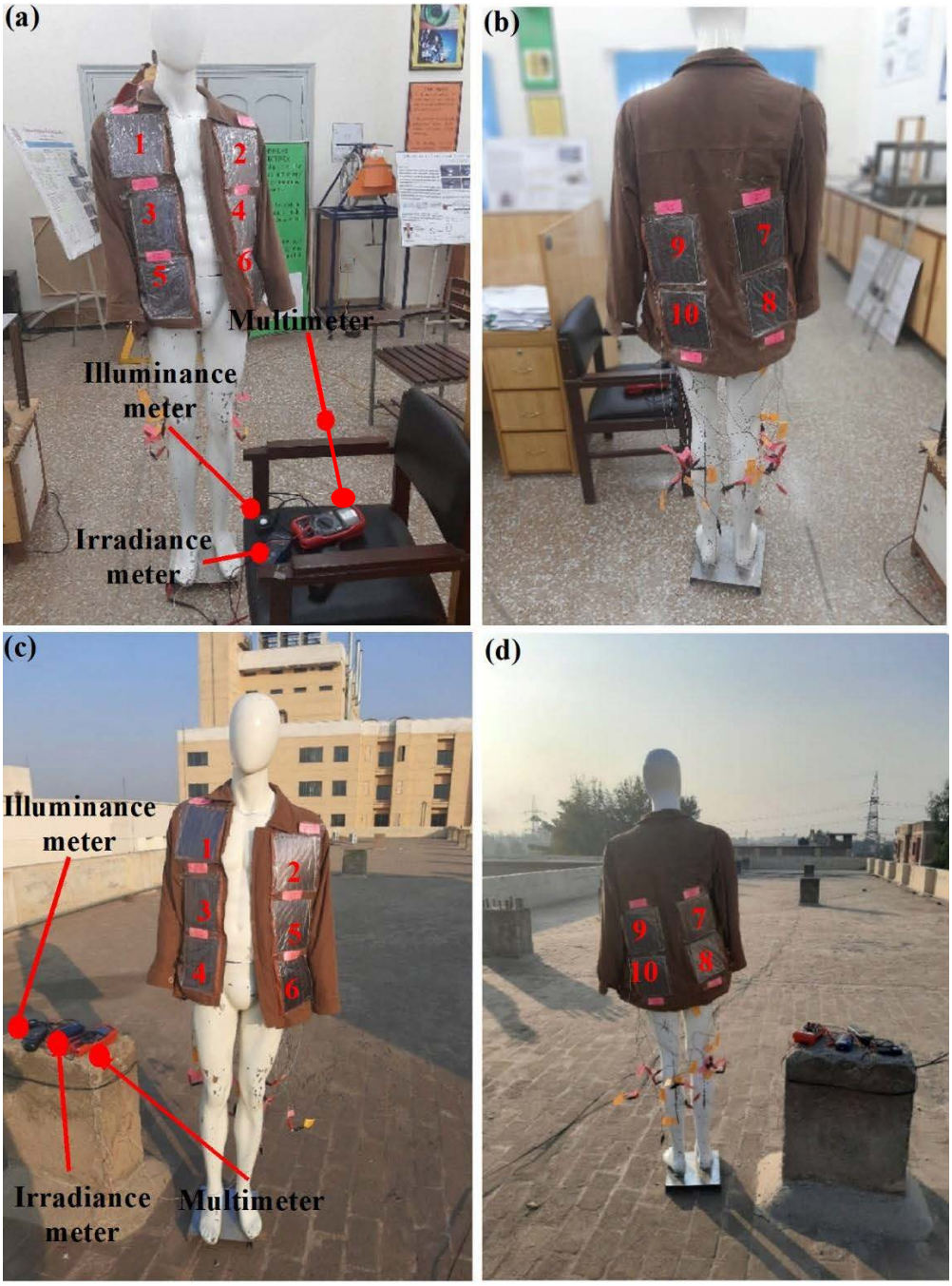

FIGURE 4. Wearable SEH jacket characterization: (a) front view of jacket, in-lab testing, (b) back-view of jacket, in-lab testing, (c) front view of jacket, outdoor (rooftop) testing and (d) back-view of jacket, outdoor (rooftop) testing.

cells, as front-side of a wearable SEH jacket is exposed to window.

1) INDOOR CHARACTERIZATION OF PROTOTYPE WITH VARIABLE LOAD

During the diffused light a variable resistive load is attached to the individual solar cell and the load voltage is measured. The maximum load voltage produced as shown in figure 6(a) is 2.35 V at a load of 222 kΩ, however, the maximum power generated on front-side by solar cell-1 is shown in figure 6(b) is 0.0516 mW at an optimal load of 56 kΩ. Whereas, the maximum power during diffused light as shown in figure 6(b) is produced by solar cell-8 integrated to backside of a jacket is 0.031 mW, at an optimal load of 56 kΩ. During the testing, the Illuminance measured on front-side is 935 lux, while, irradiance measured at window is 26 W/m^2. Whereas, the irradiance is 0.6 W/m^2 on front-side of a SEH jacket. As observed the voltage on front-side of four solar cells are

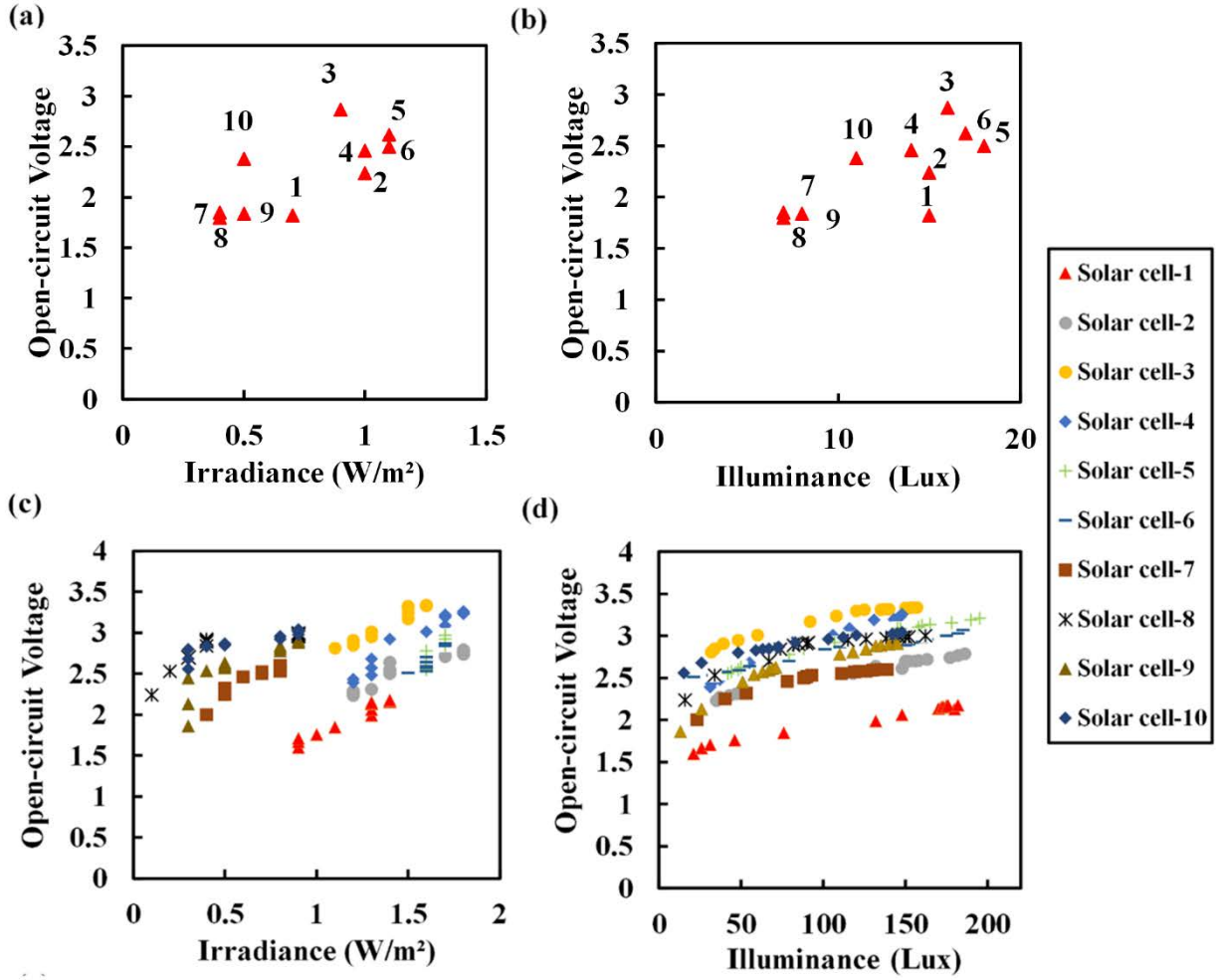

FIGURE 5. Individual solar cell output open-circuit voltage during diffused light versus (a) irradiance, (b) illuminance; (c) irradiance, indoor during turning 'ON' 1-16 tube lights and (d) illuminance, indoor during turning 'ON' 1-16 tube lights.

more than that of solar cells integrated to backside due to less illuminance and irradiance on backside of jacket facing a wall.

When 16 tube lights are turned 'ON' one by one every solar cell is characterized for the load voltage is as shown in figure 7(c). The maximum load voltage is measured to be 2.98 V and the maximum power achieved as shown in figure 7(d) is 0.728 mW at an optimal load resistance of 4.7 kΩ. The window on front side of a SEH contributed 380 lux into the light intensity, which resulted in an illuminance and irradiance recorded to be slightly less on back-side of the jacket than on front-side. Thus, the power level on back-side of a SEH jacket is 0.49 mW at an optimal load of 4.7 kΩ whereas, the illuminance and irradiance observed on back-side of jacket are 165 lux and 0.5 W/m^2, respectively which is less than the illuminance and irradiance measured on front-side of the jacket.

2) INDOOR IMPACT OF DIFFUSED AND 16 TUBE LIGHT OVER A SERIES CONNECTION WITH VARIABLE LOAD

Experiments are carried out indoor, under diffused light and variable room lightings while solar cells are connected in series. It is pertinent to mention that impact of the light from outside, entering through a window is also considered where the illuminance and Irradiance near to window was 350 lux and 12 W/m^2 respectively.

During series connection of the solar cells, the maximum load voltage and power achieved under diffused lighting conditions as shown in figure 7(a) and figure 7(b) is 8.1 V and 0.32 mW respectively. Moreover, the maximum power is produced at an optimal load resistance of 180 kΩ. During this testing, the illuminance and irradiance on front-side of the jacket was noted to be 13 lux and 1.1 W/m^2. However, the illuminance on back-side of the jacket is observed to be 5 lux, and the irradiance recorded is 0.3 W/m^2.

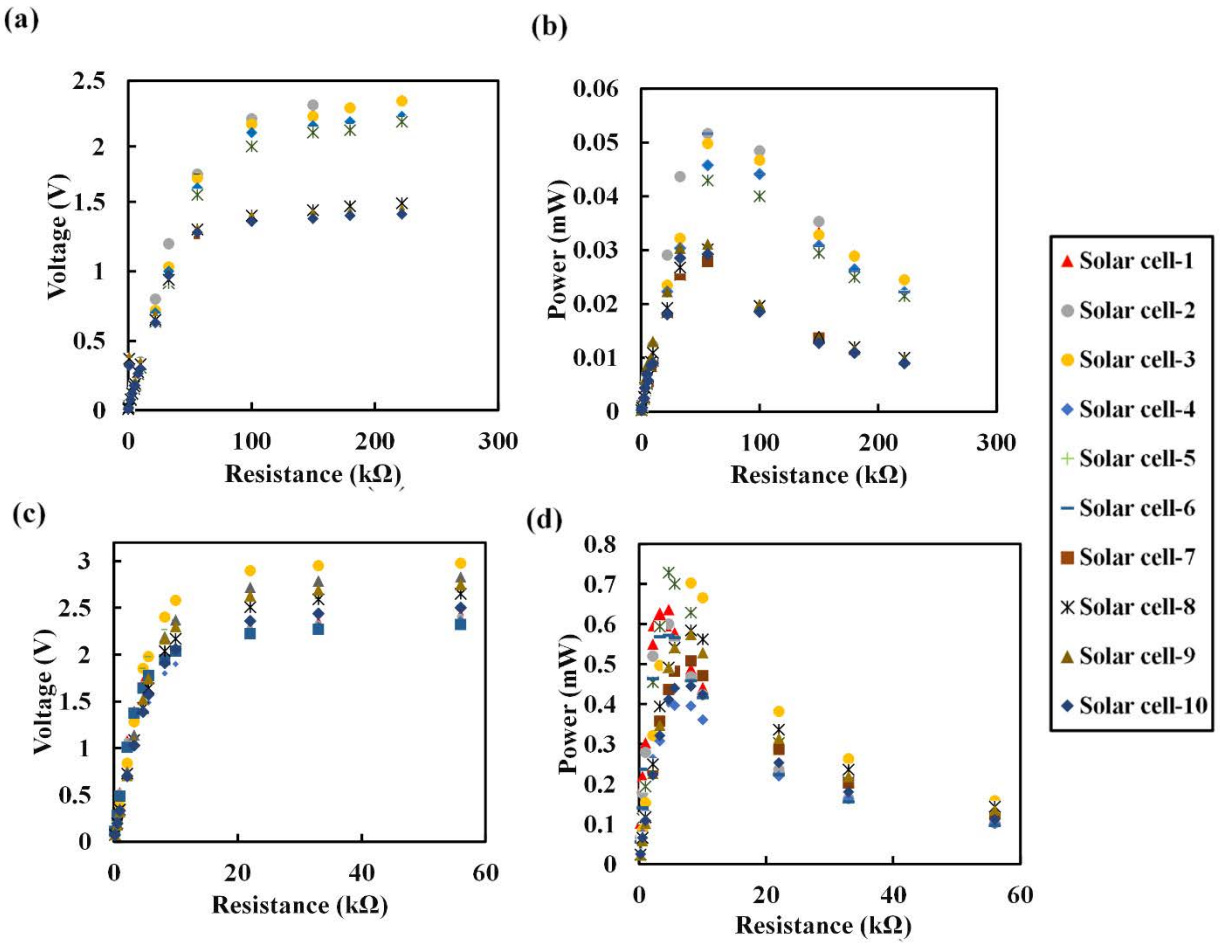

FIGURE 6. Indoor characterization of prototype individual solar cells with variable load during diffused light: (a) output voltage, (b) power (c) output voltage, indoor in 16 tube lights, and (d) power, indoor in 16 tube lights.

Similarly, indoor when 16-tube lights are turned 'ON' and the solar cells are connected in series for analysis, the maximum load voltage as shown in figure 7(c) obtained is 27.5 V at a load of 560 kΩ. The developed wearable SEH produced a maximum power of 5.689 mW at an optimum load resistance of 0.082 MΩ (figure 7(d)) is generated.On front-side of wearable SEH jacket, an illuminance is 155 lux, whereas, the irradiance is 0.9 W/m^2. While the Illuminance and irradiance on back-side is 170 lux and 0.3 W/m^2 respectively. The voltage and power levels generated from series connection during diffused and room lightings conditions from series connection of solar cells is enough to operate most of the wearable sensors, and biomedical devices.

3) OUTDOOR OPEN-CIRCUIT VOLTAGE EVALUATION OF INDIVIDUAL SOLAR CELL OF DEVELOPED PROTOTYPE

For outdoor open-circuit voltage evaluation, first all solar cells are analyzed individually. The open circuit voltage as a function of illuminance and irradiance is depicted in figure 8. In figure 8(a),the maximum open circuit voltage is produced by solar cell-1 and solar cell-3, which is measured to be 4.7 V at the illuminance of 46500 lux on front-side of wearable SEH jacket and the illuminance of 985 lux is measured near solar cell-10, which is attached to back-side of the wearable SEH jacket due to which the open circuit voltage of solar cell-10 is measured as 4.37 V, which is slightly less than the voltage levels produced by the solar cells present on the front-side of a wearable SEH jacket. Similarly, the irradiance measured on front-side near solar cell-1 is 882 W/m^2 and on solar cell-9 is 85 W/m^2. This decrease can be attributed to the direct sunlight receiving by front-side of the wearable SEH jacket.

4) OUTDOOR EVALUATION OF AN INDIVIDUAL SOLAR CELL IN A SUNNY AND CLOUDY WEATHER UNDER VARIABLE LOAD

In this case, experimentation is performed in a month of March during a sunny day. Solar cells are individually evaluated on a wearable SEH jacket for characterization and the maximum voltage produced as shown in figure 9(a) is 4.85 V, and the power level obtained as shown in figure 9(b) is 554.7 mW at an optimal load of 12 Ω at solar cell-4. The efficiency achieved during a sunny day is 5-6 %. Whereas, the illuminance on front side of wearable SEH jacket is 18700 lux and an irradiance on front side of jacket is measured, which

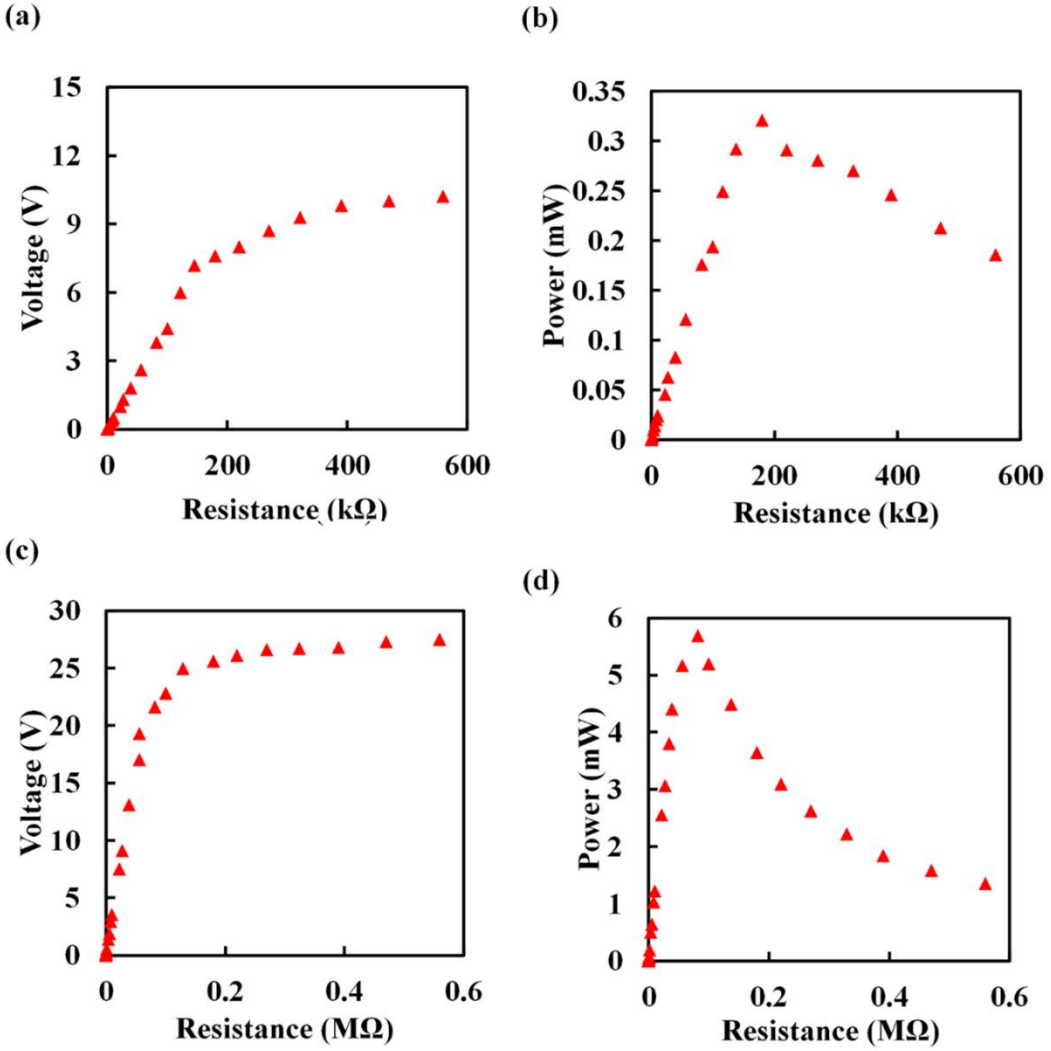

FIGURE 7. Solar cells in series connection during indoor experimentation: (a) output voltage in diffused light, (b) power during diffused light, (c) output voltage, indoor in under 16 tube lights ON, and (d) power, indoor in 16 tube lights.

happens to be 191 W/m^2 respectively. The optimal load decreases due to increase in irradiance causing a change in internal resistance of a solar cell. Moreover, on back-side of the wearable SEH jacket, the maximum voltage and power obtained by solar cell-8 is recorded to be 4.94 V and 387.56 mW at an optimal load of 22 Ω respectively. The illuminance and irradiance are recorded for back-side of the wearable SEH jacket, which is measured to be 1300 lux and 125 W/m^2 respectively.

On a cloudy day, an individual solar cell is evaluated based on voltage and power as a function of irradiance and illuminance. During experimentation, it is observed that the maximum voltage produced by cell-4 is 4.72 V at a load of 10 kΩ, and power achieved is 90.41 mW (figure 9(d)) at an optimal load of 220 Ω. While the illuminance on front-side of a wearable SEH jacket is 8250 lux whereas, irradiance on front-side is 85 W/m^2. The efficiency achieved during a cloudy weather is 1 - 1.87 %. Similarly, the maximum power which is slightly more than others solar cells on back-side of the wearable solar jacket is produced by solar cell-8 and is recorded to be 38.75 mW at an optimal load of 220 Ω and an illuminance of 1350 lux, while irradiance is 75.6 W/m^2. The optimal load resistance remained almost the same for all ten solar cells due to same irradiance around the jacket because of a cloudy weather.

5) OUTDOOR EVALUATION OF A SERIES SOLAR CELL CONNECTION WITH VARIABLE LOAD DURING VARIOUS LIGHT CONDITION

For performance evaluation of a solar cells connected in series, a wearable SEH jacket is tested and characterized outdoor in the month of March at different timings (i.e., 9 am, 4 pm, 6 pm and 8 pm). During night time the experimentation is performed for better designing of power management circuit which will harvest energy even during night time. Each experiment is performed while front-side of the wearable SEH jacket is exposed to direct sunlight.

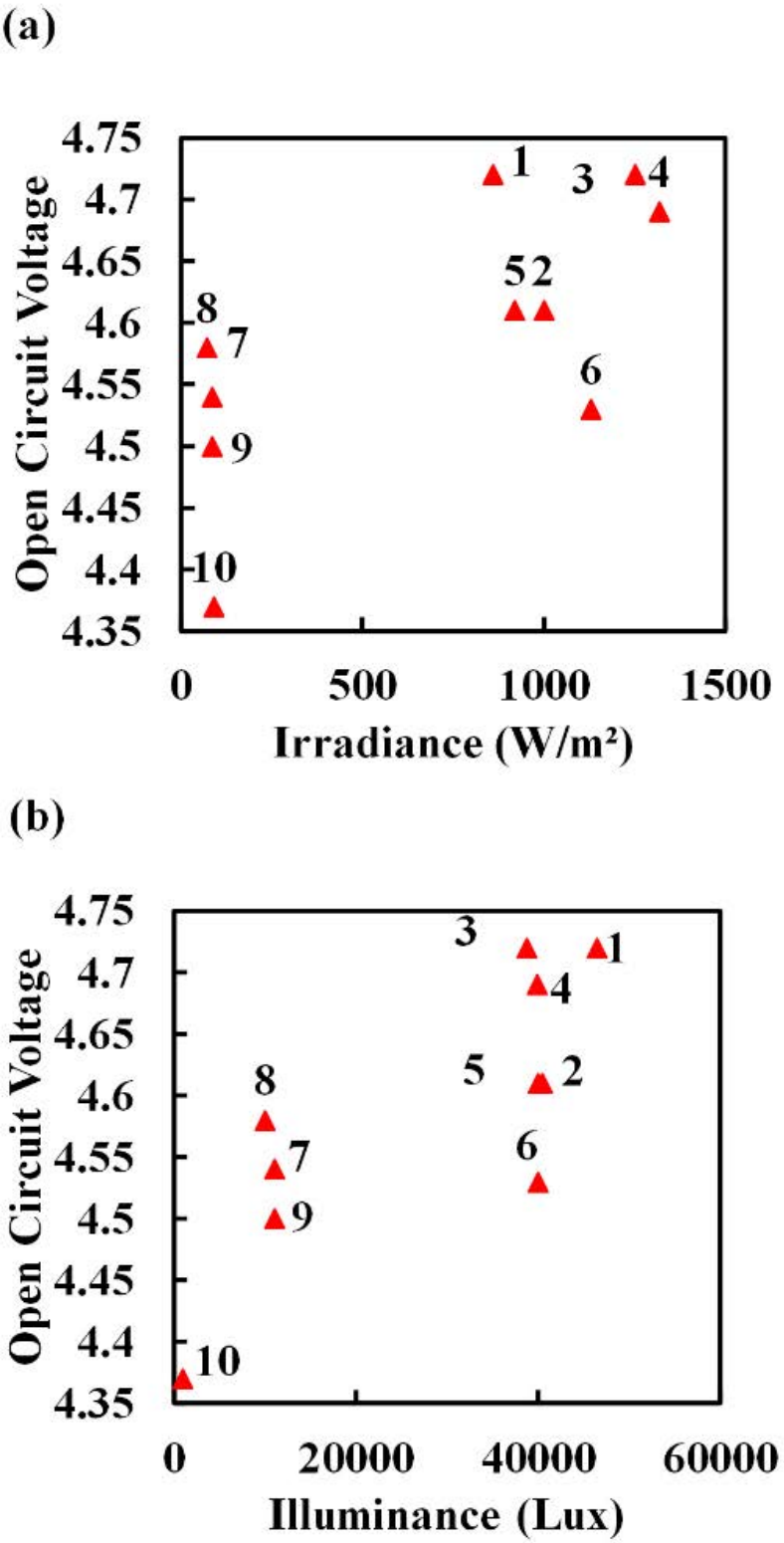

FIGURE 8. Outdoor open circuit voltage versus: (a) irradiance, and (b) illuminance.

During the testing performed at 9 am, the voltage and power produced by the SEH are depicted in figure 10(a) and figure 10(b) respectively. The voltage produced is 45 V, and the power achieved is 1282.57 mW at an optimal load of 1.5 kΩ. The power achieved is maximum due to high irradiance in an environment, as it was a sunny day. The device

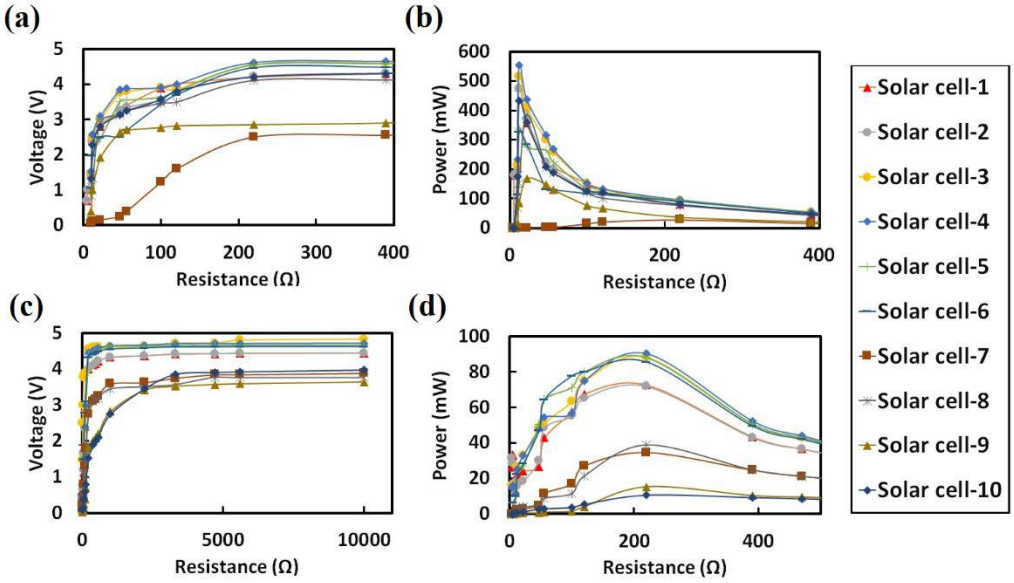

FIGURE 9. Prototype solar cells outdoor under variable load (a) output voltage, in a sunny day (b) power, in a sunny day, (c) output voltage, in a cloudy weather, and (d) power, in a cloudy weather.

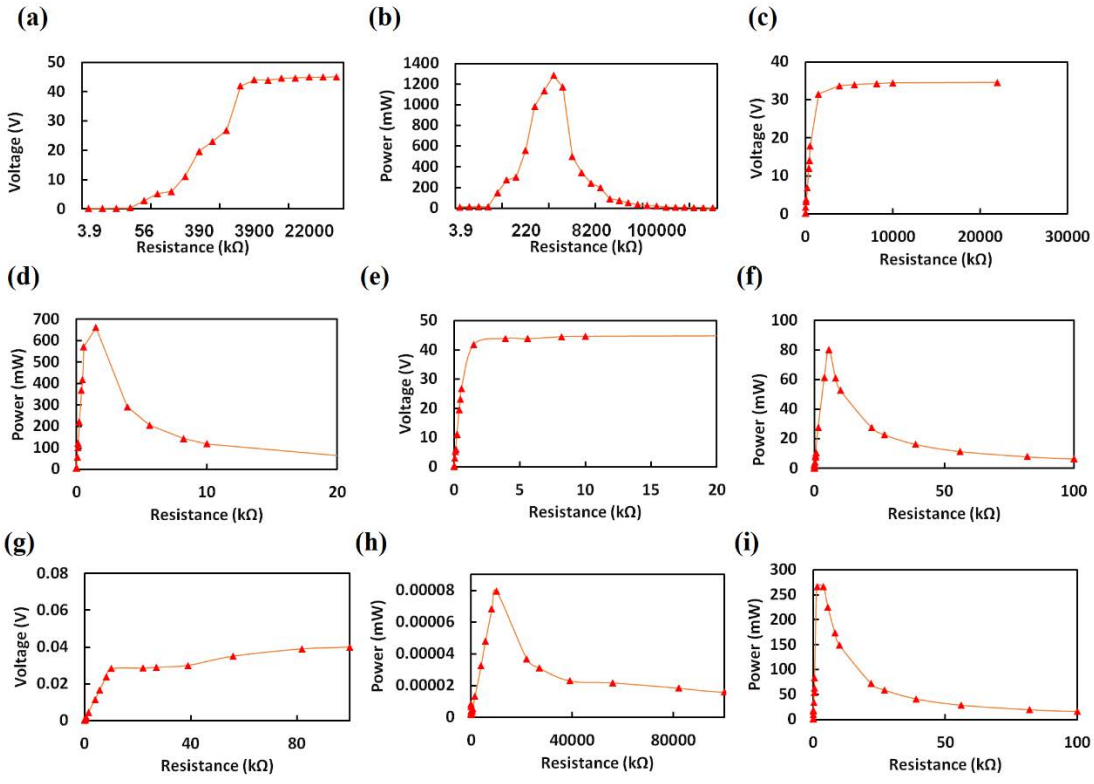

FIGURE 10. Outdoor prototype solar cells in series connection under variable load: (a) output voltage (timings: 9:00 am), (b) power (timings: 9:00 am), (c) output voltage (timings: 4:00 pm), (d) power (timings: 4:00 pm), (e) output voltage (timings: 6:00 pm), (f) power (timings: 6:00 pm), and (g) output voltage (timings: 8:00 pm), (h) output power (timings: 8:00 pm); Outdoor prototype solar cells in series connection under variable load in a cloudy weather: (i) output voltage, and (j) power.

operates as the input voltage reaches 4.3 V and instantly turn ON the Zener diode, a Darlington pair and a relay. A diode is a as discussed avoids back electromotive force caused by a relay coil, results in operation of DC-DC buck converter. As a result, battery can be charged along with powering of VHMS due to sufficient Power production. A charged battery can be later on utilized to operate a VHMS during diffused light when power production is too low.

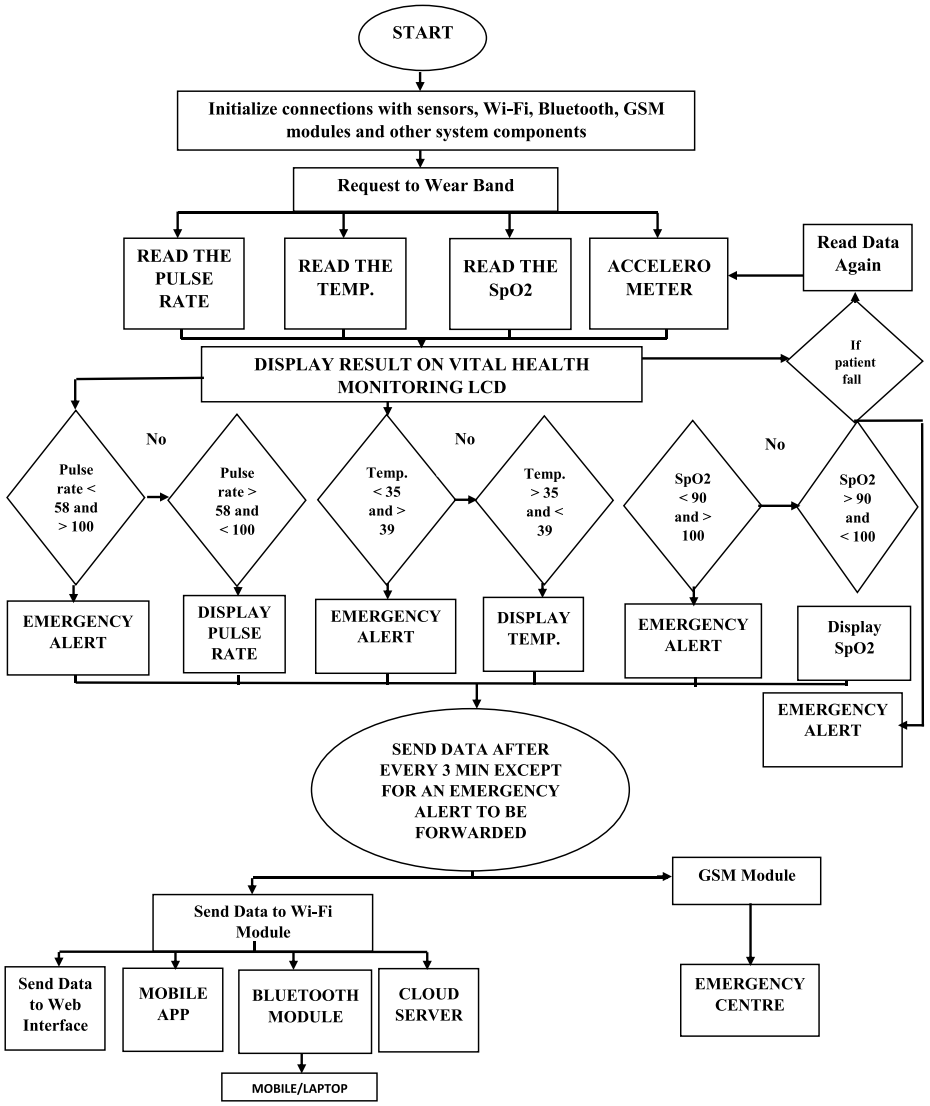

FIGURE 11. Flow chart for the functioning of a vital health monitoring system.

The irradiance and illuminance on front side of a wearable SEH jacket at 9 am is measured to be 39500 lux. Whereas, the irradiance is recorded to be 757 W/m^2. Experiments are repeated for wearable SEH jacket on backside, and the illuminance is measured to be 6200 lux and 9230 lux respectively. Due to direct sunlight on front-side of a jacket, the irradiance and illuminance on front-side of a jacket is more than on backside. In case of irradiance, on backside of wearable SEH jacket is recorded to be 139 W/m^2. It is important to mention that results obtained at 12:00 pm have not been discussed, because they are exactly similar to that of 9:00 am.

Similarly, outdoor at 4:00 pm, the solar cell evaluated achieves an output voltage of 34.8 V and power of 572.16 mW at an optimal load of 1.5 kΩ, as shown in figure 10(c) and figure 10(d) respectively. For the said reading, the illuminance is measured on front-side and backside of the jacket noted to be 34000 lux and 9100 lux respectively. Moreover, the irradiance on front-side of the wearable SEH jacket is 470 W/m^2 and on backside of the wearable SEH jacket, irradiance is measured to be 120.4 W/m^2.

In the month of March, at 6:00 pm experimentation of voltage and power of solar cells are repeated as shown in figure 10(e) and figure 10(f) respectively. As the sunset happen to decrease the light intensity due to which the illuminance on front-side is 3720 lux whereas, on backside of a wearable SEH jacket is recorded to be 3300 lux. Similarly, the irradiance is 30.5 W/m^2 and on backside it is measured to be 21.8 W/m^2. Resulted in a decrease in solar cell voltage and power to 25.6 V and 80.25 mW at a load resistance of 1.5 kΩ.

Similar experimentation is performed during night at 8:00 pm, with almost no illuminance and irradiance, the performance at night is evaluated to design a power management circuit to utilize the minute energy available in the environment, which would otherwise be wasted. Even in that case, as can be depicted in figure 10(g) and figure 10(h), the

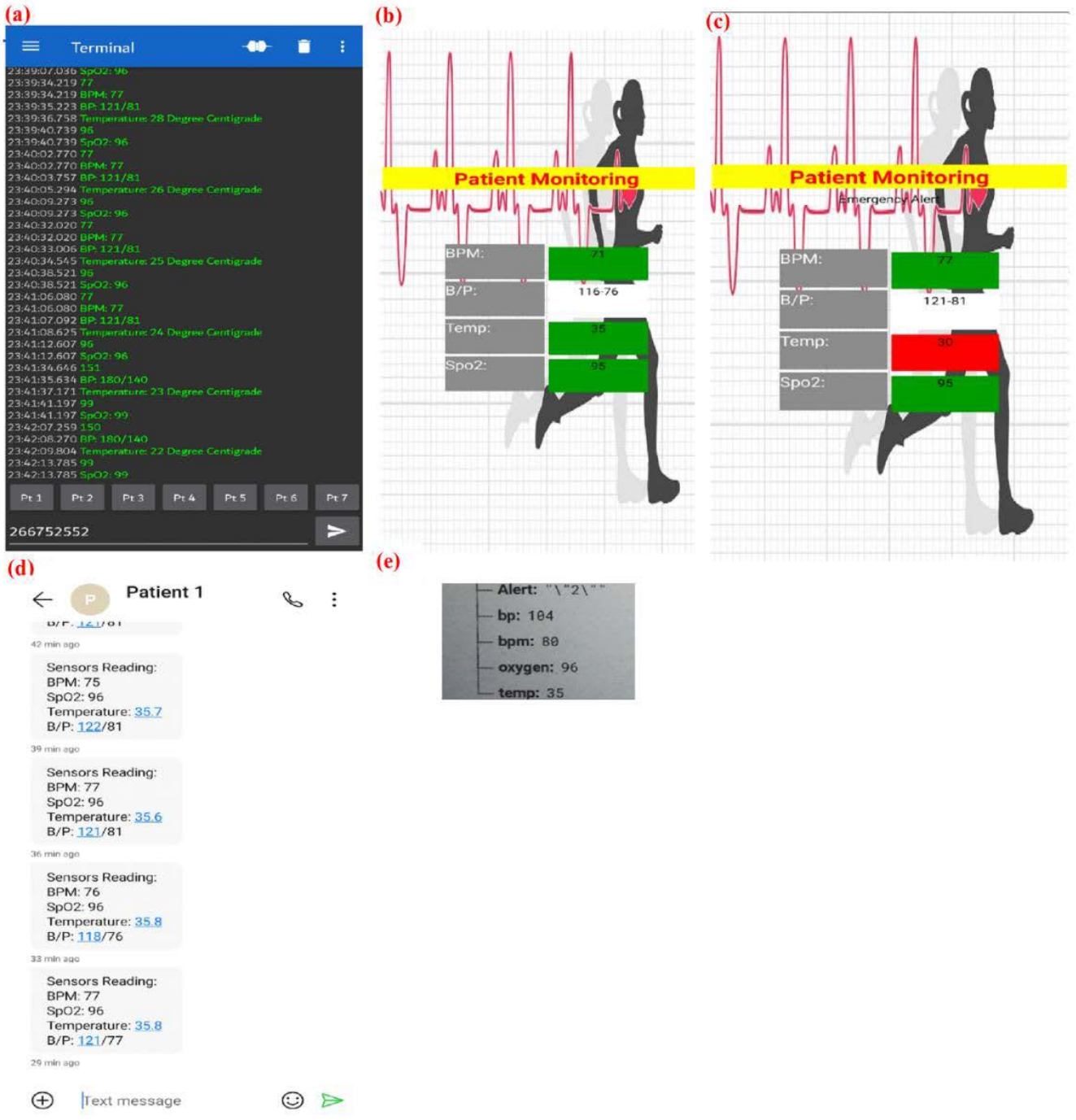

FIGURE 12. System performance evaluation through (a) Bluetooth window terminal, (b) patient monitoring mobile app, (c) emergency sound alert for temperature, (d) web real time database, and (e) GSM mobile message.

voltage and power produced are 62 mV and 7.95×10^{-5} mW (at load of 10 kΩ) respectively.

Figure 10(i) depicts the output voltage obtained is 40.4 V and the maximum power attained (figure 10(j)) is 266.66 mW at an optimal load of 1.5 kΩ. During the recorded readings, the outdoor illuminance for a series cell configuration is measured in the afternoon of 2nd March on a cloudy day over the front-side and back-side of the wearable SEH jacket. As the voltage and power are dependent on the irradiance, so the irradiance and illuminance are observed as well for the evaluation of voltage and power performance of a solar cell. On front-side, the illuminance is 4300 lux. Similarly, illuminance on backside of the wearable SEH is measured to be 7750 lux. Whereas, the irradiance on front-side of the

TABLE 6. Comparison of Solar Energy Harvester harvesting models.

Proposed solar energy harvester model	Irrad. (W/m^2)	Weather Condition considered	PWM/MPPT	Super capacitor/ Battery	Efficiency	Simulation/ Real time experimentation	Ref.
Boost Converter with MPPT	20- 1000	No	MPPT	Battery	High	Simulation	[54]
Boost Converter with MPPT		No	MPPT	Both	High	Simulation	[55]
Boost Converter		No		Battery	High	Simulation	[56]
Buck-Boost Converter with MPPT		No	MPPT	Battery		Real time experimentation	[57]
Buck-Boost Converter with Pulse width modulation (PWM) and MPPT	200-5000	Yes	PWM/MPPT	Both		Real time experimentation	[58]
Buck-Boost Converter with MPPT	0.1-780	Yes	MPPT	Battery	High	Real time experimentation	This work

wearable SEH jacket is 31 W/m^2. Moreover, on backside of the wearable SEH jacket, irradiance is measured to be 47.6 W/m^2.

V. SOFTWARE IMPLEMENTATION IN WEARABLE JACKET

The flow chart of the functioning of a vital health monitoring system (VHMS) is illustrated in figure 11. At first, the Arduino initialize connections with Wi-Fi, GSM, Bluetooth modules and sensors. Then, after wearing a band, data of pulse rate, temperature, oxygen saturation and human fall update is received from respective sensors and the information is presented on the VHMS display screen. Afterward, the data from the subject will be sent after every 3 min to Wi-Fi and GSM modules. Moreover, the measured information is further communicated to web interface, mobile app, and cloud server and to Bluetooth module through Wi-Fi module. Moreover, in case of emergency, an emergency alert of a subject health deterioration will be forwarded urgently. Furthermore, the system will provide observation of a subject inside a room, nearby place as well far distance location.

A. SYSTEM PERFORMANCE EVALUATION AND ANALYSIS

The system performance is evaluated based on the operation and functioning of the integrated modules and is configured to send the data to mobile or computer after every 3 min. The data collected by sensors is transferred to Bluetooth (figure 12(a)), mobile app (figure 12(b)), GSM mobile message (figure 12(d)) and web real time database (figure 12(e)). As can be seen in figure 12(c), when a temperature value is not in normal range an emergency alert alarm is turned 'ON' the mobile app, as well as the value on mobile app has turned into red color. Similarly, BPM, SpO_2 value will also turn red with an emergency alert. Moreover, for fall alert a sound buzzer is turned ON in case of mobile app, moreover, an alert is sent to Bluetooth and GSM module as well.

A comparison of solar energy harvesting models based on proposed model, irradiance, weather condition, efficiency and type of testing is shown in Table 6. Similarly, other researchers in [54] and [58] have varied the irradiance, while, only [58] considered weather condition on the performance. Furthermore, battery/super capacitor for charging is considered in proposed SEH, as in [54], [55], [56], [57], [58], Efficiency reported in [54], [55], [56] is high similar to the proposed device. Whereas, experimental validation of the SEH is only proposed in this work and [58].

VI. CHARGING AND DISCHARGING OF A BATTERY

A 1.2 V, 1000 mAh four batteries connected in series has an initial voltage of 0.7 V, which develops a voltage of 4.1 V in nearly 11 min, whereas, 4.8 V is achieved in 200 min. While, the display of VHMS works for 120 min, after which the display started to blink while the transmission further continued for 60 more minutes. Both the charging and discharging of the VHMS Is shown in figure 13 (a) and figure 13 (b).

VII. COMPARATIVE ANALYSIS

A comprehensive comparison of the developed prototype system with the reported related work in the literature is shown in Table 7. The solar-based VHMS gadgets are assessed based on material type (flexible/rigid), modes of communication,

TABLE 7. Comparison of wearable SEHs.

Brand	Type	Size (cm^2)	Illuminance (lux)	Voltage (V)	Power (mW)	Power density (mW/cm^2)	Modes to of communication	Sensors operated	Ref.
Sundance Solar	Flexible	43.2		5.08	127.8	2.95*		PPG and Accelerometer	[36]
PowerFilm (SP3-12)	Flexible	8.128	10000	3	18	2.21*	Bluetooth	Pulse Oxymeter	[37]
Solar Capture Technologies	Flexible	20.24		5.14	43.4	2.14*			[38]
PowerFilm (SP3-12)	Flexible	8.128		3	16	1.96*		Electromyography	[39]
Sundance Solar (MP3-37)	Flexible			3	120.7		Bluetooth	Pulse Sensor	[40]
Sundance Solar MPT3.6−75	Flexible	43.2	320	3.6	0.77	0.017*			[41]
1-dimensional perovskite solar cells	Flexible	0.05		0.91				Electric watch	[42]
This work[a]	Flexible	244.55	41000	45	1282.57	5.25*	Bluetooth, GSM and Wi-Fi	PPG sensor, Temperature, accelerometer	[This work]

a- **Irradiance = 780 W/m²**
* **Calculated**

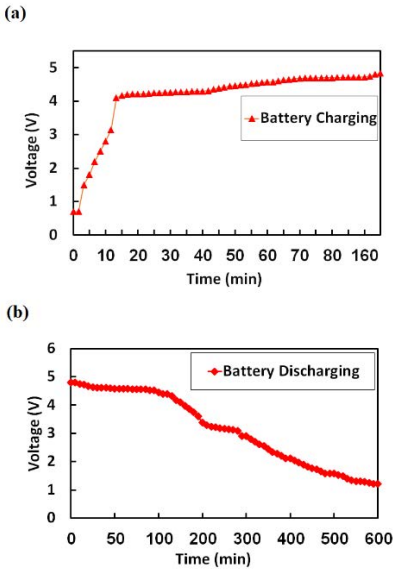

FIGURE 13. Battery (a) Charging and (b) Discharging.

sensors' power, size, voltage, power and power density. The size of SEH has a significant effect on power generation; with larger harvester's size, more power can be produced as can be concluded from [36] and [42]. Power generation capability decreases with smaller size of flexible SEH [37] and [39]. The developed SEH produces more power than any reported solar-based health monitoring system. As reported in table 7, recently developed prototypes comprise of a single solar cell whereas, the proposed device utilizes the jacket area for maximum power generation. Thus, during the daytime extra energy is stored and further utilized by the VHMS at night. The solution results in a power generation 10 times more than [40].

Furthermore, the developed solar-based VHMS produces maximum power than any reported prototype to our best knowledge.

In the works reported in literature, the sensors used for VHMS are photo plethysmography (PPG) and accelerometer in [36], Pulse Oximeter [37], Electromyography (EMG) [39], Pulse Sensor [40] and electric watch [42]. Whereas, the emergence of wearable biosensors used to extract the human parameters such as fall of the temperature, temperature, and pulse rate and oxygen saturation level. Then the data is analyzed through Bluetooth [37], [40], Global System for Mobile Communications (GSM) and Internet of Things (IoT) subsystem; the parameters are also measured and communicated to the caregiver and doctor through mobile Application.

VIII. CONCLUSION

In summary, we have developed a wearable flexible solar-based wearable jacket retaining the flexibility, deformability, and production of maximum power from natural and artificial light. The proposed SEH can power pulse sensor, oxygen saturation sensor, temperature sensor, and fall alert sensor data is fetched and then transferred to mobile app, Bluetooth terminal, web database and a mobile message through Wi-Fi, GSM and Bluetooth module. Both Vital health monitoring system design and overall maximum power point tracking (MPPT) design are crucial in order to achieve robust and power efficient device. All three level of design are discussed by demonstrating a flexible SEH power generation potential as well as analyzing the relationships between irradiance, illuminance, variable load, efficient MPPT circuit design, and optimized algorithm for efficient power use. Experimental result shows that outdoor evaluation of a series solar cell connection with variable load during different environments produced a maximum voltage produced is 45 V and power generated is 1282.57 mW, under illuminance and irradiance of 41000 lux and 780 W/m^2, respectively, at an optimal load resistance of 1.5 kΩ. Similarly, during night, with almost no illuminance and irradiance, the performance at night evaluated to design a power management circuit to utilize the minute energy available in the environment, which would otherwise be wasted. In that case the voltage and power produced are 62 mV and 7.95×10^{-5} mW (at load of 10 kΩ) respectively

CONFLICT OF INTEREST

The authors declare that there is no conflict of interest regarding the publication of this paper

ACKNOWLEDGMENT

The authors would like to acknowledge Sensors and Energy Harvesting Systems Research Laboratory (SEHSR Lab), Department of Mechatronics Engineering, University of Engineering and Technology, Peshawar, Pakistan.

REFERENCES

[1] *An Overview of Wearables Market to be Worth 25 Dollars Billion by 2019*, CCS Insight, London, U.K., 2016. Accessed: Dec. 31, 2021.
[2] A. S. Khan and F. U. Khan, "Experimentation of a wearable self-powered jacket harvesting body heat for wearable device applications," *J. Sensors*, vol. 2021, pp. 1–22, Dec. 2021, doi: 10.1155/2021/9976089.
[3] S. Li, D. Son, J. Kim, Y. B. Lee, J.-K. Song, S. Choi, D. J. Lee, J. H. Kim, M. Lee, T. Hyeon, and D.-H. Kim, "Transparent and stretchable interactive human machine interface based on patterned graphene heterostructures," *Adv. Funct. Mater.*, vol. 25, no. 3, pp. 375–383, Jan. 2015, doi: 10.1002/adfm.201402987.
[4] T. Page, "A forecast of the adoption of wearable technology," *Int. J. Technol. Diffusion*, vol. 6, no. 2, pp. 12–29, Apr. 2015, doi: 10.4018/IJTD.2015040102.
[5] H. Huang and A. V. Savkin, "An energy efficient approach for data collection in wireless sensor networks using public transportation vehicles," *AEU-Int. J. Electron. Commun.*, vol. 75, pp. 108–118, May 2017, doi: 10.1016/j.aeue.2017.03.012.
[6] L.-Q. Tao, H. Tian, Y. Liu, Z.-Y. Ju, Y. Pang, Y.-Q. Chen, D.-Y. Wang, X.-G. Tian, J.-C. Yan, N.-Q. Deng, Y. Yang, and T.-L. Ren, "An intelligent artificial throat with sound-sensing ability based on laser induced graphene," *Nature Commun.*, vol. 8, no. 1, p. 14579, Apr. 2017, doi: 10.1038/ncomms14579.
[7] C. Beach and A. J. Casson, "Inertial kinetic energy harvesters for wearables: The benefits of energy harvesting at the foot," *IEEE Access*, vol. 8, pp. 208136–208148, 2020, doi: 10.1109/ACCESS.2020.3037952.
[8] F. Shaikh, M. A. Meghani, V. Kuvar, and S. Pappu, "Wearable navigation and assistive system for visually impaired," in *Proc. 2nd Int. Conf. Trends Electron. Informat. (ICOEI)*, May 2018, pp. 747–751, doi: 10.1109/ICOEI.2018.8553690.
[9] (2017). *A Brief Overview of Wearable Technology Market—Global Opportunity Analysis and Industry Forecast, 2014–2022*. Accessed: Dec. 31, 2021. [Online]. Available: http://www.prnewswire.com/news-releases
[10] *Motorola Watch 2016 a Brief Overview of Motorola Moto 360*. Accessed: Dec. 31, 2021. [Online]. Available: https://www.motorola.com/us/products/ moto-360
[11] *Huawei Watch 2016 a Brief Overview of Huawei Watch*. Accessed: Dec. 31, 2021. [Online]. Available: http://consumer.huawei.com/en/wearables/huaweiwatch/index.htm
[12] *Fitbit 2016 an Overview of Wearable Fitbit Watch*. Accessed: Dec. 31, 2021. [Online]. Available: https://www.fitbit.com/au
[13] *Mi Band 2016 an Overview of Wearable Mi Band Watch*. Accessed: Dec. 31, 2021. [Online]. Available: http://www.mi.com/en/miband2
[14] *Google Glass 2016 an Over View of Google Glass*. Accessed: Dec. 31, 2021. [Online]. Available: https://www.google.com/glass/tech-specs/
[15] *Recon Jet 2015 an Overview of Recon Jet*. Accessed: Dec. 31, 2021. [Online]. Available: https://www.bikeradar.com/reviews/bikes/road-bikes/recon-jet-review/
[16] (2016). *Apple Airpods 2016 an Overview on Apple Airpods*. Accessed: Dec. 31, 2021. [Online]. Available: http://www.apple.com/au/airpods
[17] *Bellabeat Leaf 2016 an Overview on Bellabeat Leaf*. Accessed: Dec. 31, 2021. [Online]. Available: https://www.bellabeat.com
[18] *Eric Mack 2015 an Overview on MYO Gesture Control Armband*. Accessed: Dec. 31, 2021. [Online]. Available: https://newatlas.com/myo-gesture-control-armband-review/39103/
[19] *Lechal Footwear 2016 an Overview on Lechal Footwear*. Accessed: Dec. 31, 2021. [Online]. Available: https://lechal.com/
[20] A. S. Khan and F. Khan, "A survey of wearable energy harvesting systems," *Int. J. Energy Res.*, vol. 46, no. 3, pp. 1–53, 2021, doi: 10.1002/er.7394.
[21] J. Xiong, M.-F. Lin, J. Wang, S. L. Gaw, K. Parida, and P. S. Lee, "Wearable all-fabric-based triboelectric generator for water energy harvesting," *Adv. Energy Mater.*, vol. 7, no. 21, Nov. 2017, Art. no. 1701243, doi: 10.1002/aenm.201701243.
[22] V. Leonov, "Thermoelectric energy harvesting of human body heat for wearable sensors," *IEEE Sensors J.*, vol. 13, no. 6, pp. 2284–2291, Jun. 2013, doi: 10.1109/JSEN.2013.2252526.
[23] F. Khan and Izhar, "Piezoelectric type acoustic energy harvester with a tapered Helmholtz cavity for improved performance," *J. Renew. Sustain. Energy*, vol. 8, no. 5, Sep. 2016, Art. no. 054701, doi: 10.1063/1.4962027.
[24] F. U. Khan and T. Ali, "A piezoelectric based energy harvester for simultaneous energy generation and vibration isolation," *Int. J. Energy Res.*, vol. 43, no. 11, pp. 5922–5931, Sep. 2019, doi: 10.1002/er.4700.
[25] F. U. Khan and Izhar, "Modeling and simulation of a linear electromagnetic-based acoustic energy harvester under low sound pressure levels," *J. Chin. Soc. Mech. Eng.*, vol. 38, no. 3, pp. 317–329, 2017, doi: 10.29979/JCSME.
[26] F. Khan, F. Sassani, and B. Stoeber, "Copper foil-type vibration-based electromagnetic energy harvester," *J. Micromech. Microeng.*, vol. 20, no. 12, Dec. 2010, Art. no. 125006, doi: 10.1088/0960-1317/20/12/125006.
[27] F. U. Khan and M. U. Qadir, "State-of-the-art in vibration-based electrostatic energy harvesting," *J. Micromech. Microeng.*, vol. 26, no. 10, Oct. 2016, Art. no. 103001, doi: 10.1088/0960-1317/26/10/103001.
[28] M. A. Ullah, R. Keshavarz, M. Abolhasan, J. Lipman, K. P. Esselle, and N. Shariati, "A review on antenna technologies for ambient RF energy harvesting and wireless power transfer: Designs, challenges and applications," *IEEE Access*, vol. 10, pp. 17231–17267, 2022, doi: 10.1109/ACCESS.2022.3149276.
[29] T. Wu, J.-M. Redouté, and M. R. Yuce, "A wireless implantable sensor design with subcutaneous energy harvesting for long-term IoT healthcare applications," *IEEE Access*, vol. 6, pp. 35801–35808, 2018, doi: 10.1109/ACCESS.2018.2851940.
[30] S. Chalasani and J. M. Conrad, "A survey of energy harvesting sources for embedded systems," in *Proc. IEEE SoutheastCon*, Apr. 2008, pp. 442–447, doi: 10.1109/SECON.2008.4494336.

[31] P. De Mil, B. Jooris, L. Tytgat, R. Catteeuw, I. Moerman, P. Demeester, and A. Kamerman, "Design and implementation of a generic energy-harvesting framework applied to the evaluation of a large-scale electronic shelf-labeling wireless sensor network," *EURASIP J. Wireless Commun. Netw.*, vol. 2010, no. 1, Dec. 2010, Art. no. 343690, doi: 10.1155/2010/343690.
[32] T. Sanislav, G. D. Mois, S. Zeadally, and S. C. Folea, "Energy harvesting techniques for Internet of Things (IoT)," *IEEE Access*, vol. 9, pp. 39530–39549, 2021, doi: 10.1109/ACCESS.2021.3064066.
[33] K. S. Adu-Manu, N. Adam, C. Tapparello, H. Ayatollahi, and W. Heinzelman, "Energy-harvesting wireless sensor networks (EH-WSNs): A review," *ACM Trans. Sensor Netw.*, vol. 14, no. 2, pp. 1–50, May 2018, doi: 10.1145/3183338.
[34] S. Roundy, P. K. Wright, and K. S. J. Pister, "Micro-electrostatic vibration-to-electricity converters," in *Proc. ASME Int. Mech. Eng. Congr. Expo. Microelectromech. Syst.* New Orleans, LA, USA: ASME International Mechanical Engineering Congress and Exposition, 2002, pp. 487–496, doi: 10.1115/IMECE2002-39309.
[35] S. A. Hashemi, S. Ramakrishna, and A. G. Aberle, "Recent progress in flexible-wearable solar cells for self-powered electronic devices," *Energy Environ. Sci.*, vol. 13, no. 3, pp. 685–743, 2020, doi: 10.1039/C9EE03046H.
[36] T. Wu, M. S. Arefin, J.-M. Redoute, and M. R. Yuce, "Flexible wearable sensor nodes with solar energy harvesting," in *Proc. 39th Annu. Int. Conf. IEEE Eng. Med. Biol. Soc. (EMBC)*, Jeju, South Korea, Jul. 2017, pp. 3273–3276, doi: 10.1109/EMBC.2017.8037555.
[37] P. Jokic and M. Magno, "Powering smart wearable systems with flexible solar energy harvesting," in *Proc. IEEE Int. Symp. Circuits Syst. (ISCAS)*, Baltimore, MD, USA, May 2017, pp. 1–4, doi: 10.1109/ISCAS.2017.8050615.
[38] A. Satharasinghe, T. Hughes-Riley, and T. Dias, "An investigation of a wash-durable solar energy harvesting textile," *Prog. Photovolt., Res. Appl.*, vol. 28, no. 6, pp. 578–592, Jun. 2020, doi: 10.1002/pip.3229.
[39] V. Kartsch, S. Benatti, M. Mancini, M. Magno, and L. Benini, "Smart wearable wristband for EMG based gesture recognition powered by solar energy harvester," in *Proc. IEEE Int. Symp. Circuits Syst. (ISCAS)*. Florence, Italy: IEEE, May 2018, pp. 1–5, doi: 10.1109/ISCAS.2018.8351727.
[40] T. Wu, M. S. Arefin, J.-M. Redoute, and M. Yuce, "A solar energy harvester with an improved MPPT circuit for wearable IoT applications," in *Proc. 11th Int. Conf. Body Area Netw.* Turin, Italy: EAI, 2017, pp. 166–170, doi: 10.4108/eai.15-12-2016.2267622.
[41] W. Y. Toh, Y. K. Tan, W. S. Koh, and L. Siek, "Autonomous wearable sensor nodes with flexible energy harvesting," *IEEE Sensors J.*, vol. 14, no. 7, pp. 2299–2306, Jul. 2014, doi: 10.1109/JSEN.2014.2309900.
[42] L. Qiu, S. He, J. Yang, F. Jin, J. Deng, H. Sun, X. Cheng, G. Guan, X. Sun, H. Zhao, and H. Peng, "An all-solid-state fiber-type solar cell achieving 9.49% efficiency," *J. Mater. Chem. A*, vol. 4, no. 26, pp. 10105–10109, 2016, doi: 10.1039/c6ta03263j.
[43] G. M. Masters, *Renewable and Efficient Electric Power Systems*, 2nd ed. Hoboken, NJ, USA: Wiley, 2013, doi: 10.1002/0471668826.
[44] H.-L. Tsai, C.-S. Tu, and Y.-J. Su, "Development of generalized photovoltaic model using MATLAB/SIMULINK," in *Proc. World Congr. Eng. Comput. Sci.*, San Francisco, CA, USA, 2008, pp. 1–6.
[45] M. S. Alamri, "Modelling of photovoltaic module and experimental determinaton of serial resistance," *J. Taibah Univ. Sci.*, vol. 2, no. 1, pp. 94–105, 2009, doi: 10.1016/S1658-3655(12)60012-0.
[46] X. H. Nguyen and M. P. Nguyen, "Mathematical modeling of photovoltaic cell/module/arrays with tags in MATLAB/simulink," *Environ. Syst. Res.*, vol. 4, no. 1, Dec. 2015, Art. no. 24, doi: 10.1186/s40068-015-0047-9.
[47] H. Bellia, R. Youcef, and M. Fatima, "A detailed modeling of photovoltaic module using MATLAB," *NRIAG J. Astron. Geophys.*, vol. 3, no. 1, pp. 53–61, Jun. 2014, doi: 10.1016/j.nrjag.2014.04.001.
[48] C. Hansen. (2015). *Parameter Estimation for Single Diode Models of Photovoltaic Modules*. [Online]. Available: https://www.osti.gov/, doi: 10.2172/1177157.
[49] A. Senturk and R. Eke, "A new method to simulate photovoltaic performance of crystalline silicon photovoltaic modules based on datasheet values," *Renew. Energy*, vol. 103, pp. 58–69, Apr. 2017, doi: 10.1016/j.renene.2016.11.025.
[50] K.-I. Ishibashi, Y. Kimura, and M. Niwano, "An extensively valid and stable method for derivation of all parameters of a solar cell from a single current-voltage characteristic," *J. Appl. Phys.*, vol. 103, no. 9, May 2008, Art. no. 094507, doi: 10.1063/1.2895396.
[51] H. Ibrahim and N. Anani, "Variations of PV module parameters with irradiance and temperature," *Energy Proc.*, vol. 134, pp. 276–285, Oct. 2017, doi: 10.1016/j.egypro.2017.09.617.
[52] H. Maammeur, A. Hamidat, and L. Loukarfi, "A numerical resolution of the current-voltage equation for a real photovoltaic cell," *Energy Proc.*, vol. 36, pp. 1212–1221, Oct. 2013, doi: 10.1016/j.egypro.2013.07.137.
[53] SANYO Amorton Corporate Limited. *Amorphous Silicon Solar Cells Specification AT-7963A*. Accessed: Jan. 2022. [Online]. Available: https://docs.rs-online.com/028e/0900766b810cdd9b.pdf
[54] D. Dondi, A. Bertacchini, D. Brunelli, L. Larcher, and L. Benini, "Modeling and optimization of a solar energy harvester system for self-powered wireless sensor networks," *IEEE Trans. Ind. Electron.*, vol. 55, no. 7, pp. 2759–2766, Jul. 2008, doi: 10.1109/TIE.2008.924449.
[55] D. Brunelli, C. Moser, L. Thiele, and L. Benini, "Design of a solar-harvesting circuit for batteryless embedded systems," *IEEE Trans. Circuits Syst. I, Reg. Papers*, vol. 56, no. 11, pp. 2519–2528, Nov. 2009, doi: 10.1109/TCSI.2009.2015690.
[56] A. Castagnetti, A. Pegatoquet, C. Belleudy, and M. Auguin, "A framework for modeling and simulating energy harvesting WSN nodes with efficient power management policies," *EURASIP J. Embedded Syst.*, vol. 2012, no. 1, Dec. 2012, Art. no. 8, doi: 10.1186/1687-3963-2012-8.
[57] A. S. Weddell, G. V. Merrett, and B. M. Al-Hashimi, "Ultra low-power photovoltaic MPPT technique for indoor and outdoor wireless sensor nodes," in *Proc. IEEE Conf. Design, Automat. Test Eur.*, Grenoble, France, Mar. 2011, pp. 14–18.
[58] H. Sharma, A. Haque, and Z. Jaffery, "Modeling and optimisation of a solar energy harvesting system for wireless sensor network nodes," *J. Sensor Actuator Netw.*, vol. 7, no. 3, p. 40, Sep. 2018, doi: 10.3390/jsan7030040.

ATIF SARDAR KHAN was born in Charsadda, Pakistan, in 1989. He received the bachelor's and master's degree in electrical engineering from the University of Engineering and Technology. He is currently pursuing the Ph.D. degree in energy harvesting. He was a Lecturer at the Department of Electrical Engineering, University of Engineering and Technology Peshawar, Pakistan. He has been a Lecturer with the Department of Renewable Energy Engineering, University of Engineering and Technology Peshawar, Pakistan, since January 2020. His current research interests include comprise of energy harvesting, power management, sensors, and wearable electronic.

FARID ULLAH KHAN was born in Nowshera, Pakistan, in 1971. He received the bachelor's and master's degrees (Hons.) in mechanical engineering from the University of Engineering and Technology, Peshawar, Pakistan, in 1997 and 2004, respectively, and the Ph.D. degree in mechanical engineering from The University of British Columbia, Vancouver, Canada, in 2011. During the Ph.D. studies his field of interest was micro electro mechanical systems (MEMS), vibration based Electromagnetic energy harvester for MEMS devices, energy harvesting from sinusoidal, and random vibrations. He joined as a Lecturer at the Department of Mechanical Engineering, University of Engineering and Technology, Peshawar, Pakistan. From 2002 to 2006, he was an Assistant Professor at the Department of Mechanical Engineering. Currently, he is a Professor with the Department of Mechatronics Engineering, University of Engineering and Technology Peshawar, Pakistan. His research interests include comprise of Micro/Nano electromechanical systems (MEMS/NEMS), Low cost microfabrication technology, microelectronics, sensors and actuators, vibration-based energy harvesting, electromagnetic energy harvesting, random vibrations, modeling of linear and nonlinear harvesters, embedded sensors, piezoelectric, electrostatic and acoustic devices, micro-hydro turbines, water wheels, pumps, power plants, refrigeration, biomedical devices, prosthetics, and orthotics. He received the Presidential Gold Medal and the University Gold Medal for his distinction and extraordinary performance during his undergraduate studies. During his Ph.D. studies in The University of British Columbia, Vancouver, Canada, he also received the Just Dissert Award 2009, the UBC Alma Mater Society and GSS Appreciation Award 2011, and the Graduate Student Society UBC Vancouver for his role and contribution towards the betterment of Graduate Student Society UBC Vancouver.